Design and Performance Analysis of Commercial Reflectors Attached to Three Types of PV Module

Ramy Ahmed
Benha University,
Benha, Egypt
ramy.ahmed@hu.edu.eg

Ghada Amer
Benha University,
Benha, Egypt
ghada.amer@bhit.bu.edu.eg

***Abstract*—Solar reflectors could be one of the cheapest and easiest way to increase the power generated from the PV modules. Low-cost reflecting materials are a good solution. (Less than 1$ US dollar for each square meter), the type of commercial reflector is (semi-diffuse, flexible reflector made of an aluminized PET laminate). It's lower in cost than adding more solar PV panels. After modeling a Simulink-MATLAB test module, to be derived from the real input factors. [1]. An implementation of the PV system was already done, and long-term measurements were registered for 1 year. Based on the environmental conditions in Egypt, the measured components of hourly dropped irradiance and temperature, and some other meteorological records were collected from June 2020 till May 2021. This research represents practically the differences in the power ratio of 3 types of PV modules, - (Polycrystalline, Thin film, and Monocrystalline) - before and after applying reflecting panels. The values of short circuit current I_{SC} and open-circuit voltage V_{OC} were measured under different conditions. Data can be used to validate the comparison between the theoretical and practical calculations of the output power, also to find the range of variation in the generated power for the 3 types of PV modules to be operated under the Egyptian environmental conditions. This paper founds that the measured lowest and highest average power ratio, for the total output power of PV system were (1.2157 & 1.3185 respectively) which means the total output yield power was increased by a range varies between 21%-31% referenced to the basic output.**

I. Introduction

As the electricity produced by the PV module is directly related to the intensity of light irradiance which has been received by it, a way to improve the performance of PV systems is to use cost-effective reflecting materials. Due to less cost (less than 1$ US dollar for each square meter), and simplified assembly of reflecting panels. This research proof practically the improving of efficiency of a PV cell which varies in the range of 21% to 31%. Reflectors are reflecting irradiance over the solar panel through dispersed light radiation. This is so useful especially before & after the beak irradiance time, also in the partially cloudy days, as it considerably enhances the output of the PV module**.** In addition to that, it also tends to minimize the drawbacks of hot spot development because of the focused intensity of radiation on some sections of the panel as those happened in the case of using mirrors, which does not only enhance the performance but also increases the lifetime of PV modules. Reflectors must be installed at a certain angle, to reduce shading losses and allow maintenance access. This study practically measured the potential increased in energy yield and cell temperatures and compare between the modelled system output, which was published. [1], and the practical system output. Besides, the determination of temperature increases and its effect. By the rabidly increasing of interest to enhance the generated power from solar-PV plants, promising paper and researches related to the usage of reflector surfaces attached to the PV panels are emerging. A way to discuss the simulated results of attaching a type of commercial reflector surface to the PV panels showing the best power factor of the different types of the PV panels. [1]. A paper presents the comparison of performance of a mirror reflected solar panel (MRSP) with automatic cooling and tracking [2]. Another research presents new methodologies for properly modeling PV system using a bidirectional reflectance function for non-ideal surfaces rather than traditional geometric optics. This methodology allows for the evaluation and optimization of specular and non-specular reflectors in planar con-centration systems. The energy improvement is 18% for both systems. Simulations show that a maximum increase of 30% is achievable for an optimized system located in Kingston, Canada. [3]. A comparison between two kinds of reflectors, mirror glass and aluminum foil. The result shows that, the system with mirror reflector has produced 15% higher output power. [4]. A paper provides design and performance analysis of commercial silicon based PV module with reflectors for Mumbai latitude (ϕ =19.12°). The flat reflectors made of anodized Aluminum sheet were attached to shorter sides of PV module at North-South direction. The results show that modified module produced 15% more PV power than one-sun concentration of PV module. [5]. Recent studies on light shelves found that building energy efficiency could be maximized by applying photovoltaic (PV) modules to light shelf reflectors. It was determined that PV modules should be considered in the design of light shelves as their daylighting and concentration efficiency change according to their angles. [6]. In the present work a solar collector with V-trough concentrator system were designed and fabricated with geometric concentration ratios two suns to get an extra electric output power. The experiment was carried out in Al-Zwraa Company in Baghdad. The main results indicated that the solar concentrator system caused to increase the short circuit current due to increase the amount of incident solar radiation on the solar modules, and thus increase in output power. [7]. Some researches focuses on developing a method of evaluation the effect of concentrator on the solar panel performance to get a higher power and optimum efficiency. Also using the cooling mechanism to reduce the overheating effect was discussed. The variation in maximum output power (ΔP_m) is varies between (17% - 30%) and all solar parameters increased. [8-13]. Also, the solar atlas of

ISSN 2305-7254

Egypt could be a very useful reference to validate the measured values of irradiance and temperature by comparing it with the most common average readings delivered by solar atlas. [14]. In Mirror-Augmented Photovoltaic (MAPV) systems. The system preserves its constructive simplicity with commercial flat PV modules even though dual axis tracker must be implemented, since (MAPV) systems harness mainly the direct radiation. various results were discussed. [15-20]. Results of the effect of dust on different solar mirror materials in Morocco. The highest average cleanliness drop per month for the horizontal mirrors was 45 % and 33 % for the glass and aluminum mirrors respectively. The +45° mirrors come in the second position with a cleanliness drop of about 14 % for both reflectors. [21]. A mathematical model for modelling the solar radiation components and photovoltaic arrays power outputs from arbitrarily oriented photovoltaic panel has been presented. Base on the model electrical power prediction of the photovoltaic system in realistic local condition has been presented and compared with experimental measurement. It has been shown that base on the model prediction, the efficiency and possible failures of the system can be found which are important from the technical and economical point of view. [22]. The recent developments and trends of research in laboratories and industrial achievements communicated within the last years are reviewed, and the major developments linked to alkali post deposition treatment and composition grading in CIGS. The possibility to grow thin films of large area absorber onto a glass as well as lightweight, flexible substrates opens up the field for low-cost manufacturing methods as well as new applications. [23]. A research focuses on the behavior and efficiency of a stationary CPC-PV solar collector. Each trough of this collector has different concentration factors (1.25 and 1.66) with vertically placed bi-facial cell receivers. The results showed that higher concentration factors led to larger operating temperatures (114ºC for a concentration factor of 1.66 and 96ºC for a concentration factor of 1.25). Although this may compromise the cell performance and shorten the device's life cycle, it is shown that appropriate ventilation will allow manageable operating temperatures. [24]. By utilizing optical reflectors (manufactures from aluminum metal). The important novelty of this study is the successful improvement of the electrical parameters of the on-grid PV solar system (smart grid) connected to the low tension utility grid. [25]. The impact of tilt angle is more pronounced on the thermal production than the electrical one. Furthermore, the HTF recirculation with an average temperature of 35.1˚ C and 2.2 L/min flow rate showed that the electrical yield can increase by 25%. On the other hand, by using insulation, the thermal yield increases up to 3% when working at a temperature of 23˚ C above ambient. [25].

II. Methodology and Modeling

A system of 3 types of PV panels was selected, it's an already running system, the selection of the system was based on a huge logged data which is already stored and can be used as a reference of the research.

The location of the project is in Heliopolis University campus on the top roof of the building of the Faculty of Engineering. with a location coordinates: 30°09'11.7"N 31°25'57.4"E.

Fig.1 General view of the location

A. Description of the applied system

The solar system is installed on the roof of the Heliopolis University in Cairo. Three inverters are connected to a Sunny Island System with batteries.

Installation of 4.5 kWp demo plant with different types of modules and integration of local materials for mounting structure.

1) Panels

The system consists of 3 sets of panels, each is consisting of one type of the PV, and generate an approximate power= of 1.5KW

i. Mono-Crystalline Panels:

Consisting of 8 panels, Manufacturer: SOLAR WORLD, Country: Germany, P_{max} = 175 W, V_{OC} = 44.4 V, V_{mpp} = 35.8 V, I_{SC} = 5.3 A, I_{mpp} = 4.9 A, Total Power for the panels: 1400 W.

ii. Polycrystalline Panels

Consisting of 7 panels, Manufacturer: Canadian Solar, Country: Canada, P_{max}= 235 W, V_{OC}= 36.9 V, V_{mpp}= 29.8 V, I_{SC} = 8.46 A, I_{mpp} = 7.9 A, Total Power for the panels: 1645 W

iii. Thin Film Panels

Consisting of 21 panels, Manufacturer: First Solar Country: Germany, P_{max}= 70 W, V_{OC}= 88 V, V_{mpp}= 65.5 V, I_{SC} = 1.23 A, I_{mpp} = 1.07 A, Total Power for the panels: 1470 W

Total Power of the system=1400 (Mono Crystalline) +1645 (Polycrystalline)+1470 (Thin film) = 4515 W.

A reflectance model based on a BDRF (Bidirectional Reflectance Function) for the isotropic roughened surface is developed to predict the performance of the reflector system. Fig.2 a,b.

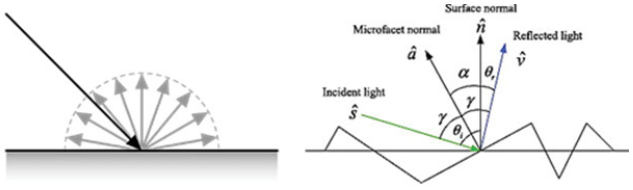

Fig.2 a Fig.2 b

(Fig. 2 a,b). Isotropic roughened surface on a BDRF model

The model methodology presented in this paper uses the concepts of the BDRF (Bidirectional Reflectance Function) of non-ideal surfaces rather than traditional geometric optics. This methodology allows for the evaluation of non-specular reflectors in planar concentration systems, which has been shown to increase the energy yields from these systems. [3]

B. Effect of temperature

While an increase in reflected irradiance is anticipated, which will increase generated electricity, it will also raise the temperature of the PV modules. The effect of higher temperatures on PV modules is that they harm the module's open-circuit voltage (V_{OC}), which will be considered in this article. [8]

PV panels, like all semiconductor products, are temperature sensitive. Temperature changes minimize a semiconductor bandgap, impacting most of the semiconductor material parameters. [9] A reduction in a semiconductor's bandgap as temperature rises can be interpreted as an increase in the energy of the material's electrons. As a consequence, less energy is required to break the bond. Reduced bond energy decreases the bandgap in the bond model of a semiconductor bandgap. As a consequence, raising the temperature decreases the band difference. [13].

1) Temperature dependence of the energy bandgap

As the temperature increases, the energy bandgap of semiconductors starts to narrow. When the magnitude of the atomic motions increases, the interatomic spacing increases, which helps to explain this phenomenon. as a result of the increased thermal energy [16]. The linear expansion coefficient of a material is used to quantify this effect. The potential is seen by electrons in the material decreases as interatomic spacing increases, decreasing the size of the energy bandgap [17]. The bandgap is increased (decreased) when the interatomic distance is directly modulated, such as by applying high compressive (tensile) stress [24].

The energy bandgap's temperature dependence has been calculated experimentally, yielding the following expression for E_g as a function of temperature T:

$$E_g(T) = E_g(0) - \frac{\alpha T^2}{T+\beta} \quad (1)$$

where E_g (0), □ and □ are the fitting parameters. These fitting parameters are listed for germanium, silicon, and gallium arsenide in Table I below: [21]

TABLE I. FITTING PARAMETERS FOR SEMICONDUCTORS

	Germanium	Silicon	GaAs
E_g (0) [eV]	0.7437	1.166	1.519
□ [eV/K]	4.77 x 10^{-4}	4.73 x 10^{-4}	5.41 x 10^{-4}
□ [K]	235	636	204

The open-circuit voltage is the parameter in PV modules that are most impacted by temperature. [22.]

The effect of rising temperatures is represented in Fig. 3.

Since I_0 is temperature dependent, the open-circuit voltage decreases with temperature. From one side of a p-n junction, the equation for I_0 is:

$$I_0 = qA\frac{Dn_i^2}{LN_D} \quad (2)$$

where:
q is the electronic charge given on the constants page;
A is the area;
D is the diffusivity of the minority carrier given for silicon as a function of doping in the Silicon Material Parameters page;
L is the minority carrier diffusion length;
N_D is the doping; and
n_i is the intrinsic carrier concentration given for silicon in the Silicon Material Parameters page.

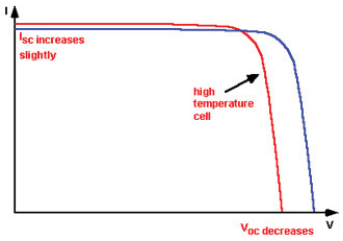

Fig.3. The effect of temperature on the IV characteristics of a solar cell

Many of the parameters in the above equation are thermodynamically favourable, but the intrinsic carrier concentration, n_i, has the most massive impact. The intrinsic carrier concentration is determined by the bandgap energy (lower bandgap energy corresponds to a significantly higher carrier concentration) and the energy that the carriers possess (with higher temperatures giving higher intrinsic carrier concentrations). The intrinsic carrier concentration can be calculated as follows: [26].

$$n_i^2 = 4\left(\frac{2\pi kT}{h^2}\right)^3 (m_e^* m_h^*)^{3/2} exp\left(-\frac{E_{Go}}{kT}\right) = BT^3 exp\left(-\frac{E_{Go}}{kT}\right) \quad (3)$$

where:
T is the temperature;
h and k are constants given in the constants page;
m_e^* and m_h^* are the effective masses of electrons and holes respectively;
E_{Go} is the band gap linearly extrapolated to absolute zero; and
B is a constant which is essentially independent of temperature.

Substituting these equations back into the expression for I_0, and assuming that the temperature dependencies of the other parameters can be neglected, gives:

$$I_0 = qA\frac{D}{LN_D} BT^3 exp\left(-\frac{E_{Go}}{kT}\right) \approx B'T^{\gamma} exp\left(-\frac{E_{Go}}{kT}\right) \quad (4)$$

Where B' is a constant that is independent of temperature. To account for the potential temperature dependencies of the other material parameters, a constant, γ, is used instead of the number 3. I_0 nearly doubles with every 10 °C rise in temperature for silicon PV panels near room temperature. By substituting the equation for I_0 into the equation for V_{OC}, as shown below, the effect of I_0 on the open-circuit voltage can be calculated:

$$V_{OC} = \frac{kT}{q} ln\left(\frac{I_{SC}}{I_O}\right) = \frac{kT}{q}[\ln I_{SC} - \ln I_O] = \frac{kT}{q}\ln I_{SC} - \frac{kT}{q} ln\left[B'T^{\gamma} exp\left(-\frac{qV_{GO}}{kT}\right)\right] = \frac{kT}{q}\left(\ln I_{SC} - \ln B' - \gamma \ln T + \frac{qV_{GO}}{kT}\right) \quad (5)$$

where $E_{Go} = qV_{GO}$. Assuming that dVoc/dT does not depend on dIsc/dT, dVoc/dT can be found as:

$$\frac{dV_{OC}}{dT} = \frac{V_{OC} - V_{GO}}{T} - \gamma\frac{k}{q} \quad (6)$$

The above equation demonstrates that a PV panel's temperature sensitivity is proportional to its open-circuit voltage V_{oc}, with higher voltage PV panels being less affected by temperature. E_{Go} is 1.2 for silicon, and setting γ to be 3 reduces the open-circuit voltage V_{oc} by around 2.2 mV/°C:

$$\frac{dV_{OC}}{dT} = -\frac{V_{GO} - V_{OC} + \gamma\frac{kT}{q}}{T} \approx -2.2mV\ per\ ℃\ for\ Si \quad (7)$$

Since the bandgap energy, E_G, decreases with temperature, more photons have enough energy to build e-h pairs, the short-circuit current, I_{SC}, increases slightly. However, this is a minor consequence, as shown in equation (8), which shows the temperature dependence of the short-circuit current from a silicon photovoltaic cell:

$$\frac{1}{I_{SC}}\frac{dI_{SC}}{dT} \approx 0 \cdot 0006\ per\ ℃\ for\ Si \quad (8)$$

or ≈0.06% per °C for silicon.

The following equation approximates the temperature dependence FF for silicon:

$$\frac{1}{FF}\frac{dFF}{dT} \approx \left(\frac{1}{V_{OC}}\frac{dV_{OC}}{dT} - \frac{1}{T}\right) \approx -0 \cdot 0015\ per\ ℃\ for\ Si \quad (9)$$

The following is the impact of changing temperature dT on maximum power output, P_M:

$$P_{Mvar} = \frac{1}{P_M}\frac{dP_M}{dT} = \frac{1}{V_{OC}}\frac{dV_{OC}}{dT} + \frac{1}{FF}\frac{dFF}{dT} + \frac{1}{I_{SC}}\frac{dI_{SC}}{dT} \quad (10)$$

$$\frac{1}{P_M}\frac{dP_M}{dT} \approx -(0 \cdot 004\ to\ 0 \cdot 005)\ per\ ℃\ for\ Si$$

or 0.4% to 0.5% per °C for silicon. (11)

C. *Effect of solar irradiance*

The predicted rise in reflected irradiance would result in an increase in generated power by increasing the PV module's short circuit current (I_{sc}). As a response to the PV module, while a higher light intensity has fallen on its surface, A positive effect on the short circuit current of the module will take place. All photovoltaic cell parameters, including the, short-circuit current, and the open-circuit voltage are affected by the amount of light incident on the cell. [23]

1) *The effect of concentration on a PV cell's IV characteristics*

The series resistance has a greater impact on cell output when the light intensity is high, while the shunt resistance has a greater impact when the light intensity is low. A solar cell short-circuit current is proportional to the light intensity, so a device operating under ten suns would have ten times the short-circuit current of a device operating under one sun. However, since incident power increases linearly with concentration, this effect does not increase the efficiency of the PV panel. Instead, the logarithmic dependence of the open-circuit voltage on the short circuit is responsible for the efficiency gains. V_{oc} increases logarithmically with light intensity under concentration, as in the equation below:

$$V'_{OC} = \frac{nkT}{q} ln\left(\frac{X\ I_{SC}}{I_O}\right) = \frac{nkT}{q}\left[ln\left(\frac{I_{SC}}{I_O}\right) + lnX\right] = V_{oc} + \frac{nkT}{q}\ln X \quad (12)$$

Where X is the concentration of sunlight.

From equation (12), a doubling of the light intensity (X=2) causes an 18 mV rise in V_{OC}.

The Sandia PV Array Performance Model (SAPM) defines five points on the IV curve. These points are shown in the Fig. 4.

$$I_{SC} = I_{SC0} * \mathcal{F}_1\left(\frac{E_b\mathcal{F}_2 + \mathcal{F}_d E_d}{E_0}\right) * \left(1 + \alpha_{Isc}(T_C - T_0)\right) \quad (13)$$

$$I_{mp} = I_{mp0}(C_0 E_e + C_1 E_e^2)\left(1 + \alpha_{Imp}(T_C - T_0)\right) \quad (14)$$

$$V_{OC} = V_{OC0} + N_s\delta ln(E_e) + \beta V_{OC}(T_C - T_0) \quad (15)$$

$$V_{mp} = V_{mp0} + C_2 N_s\delta ln(E_e) + C_3 N_s(\delta ln(E_e))^2 + \beta V_{mp}(T_C - T_0) \quad (16)$$

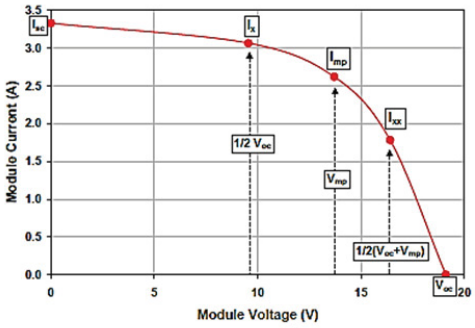

Fig.4 The SAPM defines the primary points (I_{SC}, Imp, V_{OC}, V_{mp}) with the following equations

where

- $\mathcal{F}_1$ is a 4th order polynomial function of the absolute air mass, AM_a, and is called the air mass modifier.
- $\mathcal{F}_2$ is a 5th order polynomial function of angle of incidence, AOI, and is called the angle of incidence modifier.
- E_b is beam irradiance on the plane of the array.
- E_d is the diffuse irradiance on the plane of the array.
- E_0 is reference solar irradiance (1000W/m^2).
- T_C is cell temperature (°C)
- T_0 is reference cell temperature (25 °C)
- $\mathcal{F}_d$ is the fraction of the diffuse light that is used by the module. For typical flat plate modules $\mathcal{F}_d$ is usually assumed to be equal to 1. For concentrators, the value can be smaller than 1.

- $\boldsymbol{\alpha_{Isc}}$ is the normalized temperature coefficient for short circuit current. Units are 1/ °C
- $\boldsymbol{\alpha_{Imp}}$ is the normalized temperature coefficient for maximum power current.

Units are 1/ °C

- $\boldsymbol{N_s}$ is the number of cells in series.
- $\boldsymbol{C}$ is a vector of coefficients determined by module testing using a method developed at Sandia.
- $\mathbf{E_e}$ is the "effective irradiance". It is defined as:

$$E_e = \frac{I_{sc}}{I_{sc0}\{1+\alpha I_{sc}(T_C - T_0)\}} \quad (17)$$

where:

- I_{SC0} is the short circuit current at reference conditions.
- $\boldsymbol{I_{SC}}$ can be calculated from (eq. 1) above.
- $\boldsymbol{\delta}$ is a function of T_c defined as:

$$\delta = \frac{n*k(T_c+273{\cdot}15)}{q} \quad (18)$$

where:

- $\boldsymbol{n}$ is an empirically determined 'diode factor',
- $\boldsymbol{k}$ is Boltzmann's constant (1.38066 x 10^{-23} J/K),
- $\boldsymbol{q}$ is the elementary charge constant (1.60218 x 10^{-19} Coulomb)
- $\boldsymbol{\beta V_{OC}}$ is a function of effective irradiance, E_e , defined as:

$$\beta V_{OC} = \beta V_{OC0} + m\beta V_{OC}(1 - E_e) \quad (19)$$

, where:

- $\boldsymbol{\beta V_{OC0}}$ is the temperature coefficient for module open-circuit voltage at irradiance conditions of 1000W/m^2
- $\boldsymbol{m\beta V_{OC}}$ is a coefficient describing the irradiance dependence for the open-circuit voltage temperature coefficient (typically equals zero).

A proportional dimension of planar concentrator will be installed at the open solar outdoors test field on the top roof of the Faculty of Engineering, Heliopolis University for Sustainable Development (30°09'11.7"N 31°25'57.4"E). 3 groups of PV modules were arranged in front of the wide planar reflectors, and their actual locations concerning the reflector are shown in (Fig.5&6). The tilt angles of the reflecting surfaces from horizontal were initially ø =10◦ and PV modules angles ω =30◦.

SMA Meteo Station is a device for measuring power-related meteorological data at the PV plant location and for transmitting this data to the Sunny WebBox via the Power Injector.

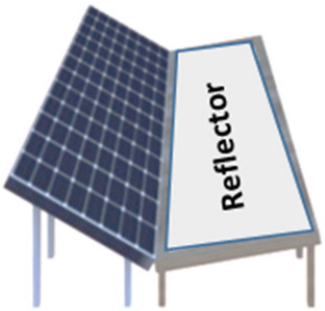

Fig.5 Proposed fixing of the reflectors

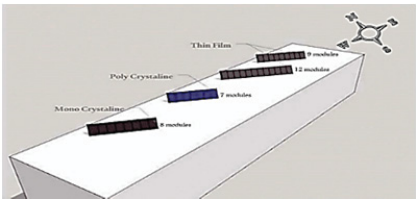

Fig.6 Orientation of the PV panels on the top roof of the building

III. Experimental Results and Discussion

A set of modules with reflectors were installed at the same module tilt angle and at a tilt angle of 30˚ to match the optimal tilt angle for the region. The reflector angle was set to be 10˚ Meteorological measurements were collected by the SMA Meteo Station.

Fig.7 SMA Meteo Station

SMA Meteo Station fulfils the following tasks:

• Measurement of global radiation
• Measurement of PV cell temperature
• Measurement of absolute air pressure
• Measurement of air temperature and humidity
• Transmission of this meteorological data to the Sunny WebBox.

All measurements were taken at the site. The modules were monitored for short-circuit current (I_{sc}) and the temperature at the top and bottom of the module. The reflector system was installed using a type of reflector: commercial reflector (semi-diffuse, flexible reflector made of an aluminized PET laminate, (Foylon). Consists of 3 layers, Polyester with a thickness (12 micro meters) + Aluminium with the thickness (7 micro meters) + Polyethylene with the thickness (80 micro meters) Commercially it's written: (Pet. / Alu. / Pe. 12/7/80 mic).

Which is preferred because of the protective layer of Polyethylene. It should be noted that both modules and reflectors should be cleaned of any major soiling and organic depositions when they were observed.

The incident illumination on reflectors is based on the sun's azimuth and elevation angle. This process was measured for the entire year to calculate the cumulative amount of annual yield power. Further calculations can be performed for different system designs (e.g., reflector tilting for other angles by simply repeating the above process). In addition to absolute power density, to obtain an optimum model configuration, the irradiance distribution on PV modules must be studied. Since the fixed PV panels were augmented by reflectors throughout the day, the occurrence of a uniform irradiance distribution on modules is expected. The uniformity

issue is an important factor to fully study power production capability and estimate degradation rates. The output generated power curves were collected from the system log files then we could use it to compare the results after using reflectors.

A. Logged data to be used

A logged data was registered to be used in comparison for both systems before and after using the reflectors.

The weather data (solar Irradiance, ambient and module temperature), and PV system instantaneous power were acquired from the weather meters (Pyrometers & Thermometer) and solar panels located at Heliopolis University for sustainable development campus, Faculty of Engineering building. The global solar irradiance, ambient temperature, module temperature, I_{PV}, V_{PV}, and specified data of output power were recorded and stored starting from year 2013 till now, the last year data 2020-2021 was measured as a calculated result from June 2020 till May 2021 with the sampling rate of one hour.

The PV model and solar model were used for the determination of the power generation from the photovoltaic panel for location coordinates: 30°09'11.7"N 31°25'57.4"E., Cairo, Egypt. In Fig.1 The local monthly average ambient temperature T base on the measurement, and, the monthly average daily solar radiation together with clearness index are presented. The PV power output directly depends on the amount of radiation incident on the surface of the PV array and array temperature.

The following are samples of the used data as the real records to be an input for the comparison to notice the output power after using the reflectors for the 3 types of PV module.

1) Total yield energy (kWh) for the year 2019 for the 3 types of modules without reflectors.
2) Total yield Energy for the year 2018 for the 3 types of modules without reflectors.
3) Average of the total yield energy for the 3 types of modules for the years 2018,2019.
4) A typical result of one day for the generated power (kW) of each of the 3 types of PV modules. Fig.8
5) Average of the total yield energy for the thin-film modules for the years 2018, 2019.
6) Average of the total yield energy for the monocrystalline modules for the years 2018, 2019 Fig.9
7) Average of the total yield energy for the Polycrystalline modules for the years 2018, 2019
8) Irradiance & ambient Temperatures results for the year 2019. Fig.10
9) Irradiance & ambient Temperatures results for the year 2018.

A MATLAB Simulink PV model was implemented with the same specs as the real PV system which was built on the top roof of the building of the Faculty of Engineering, Heliopolis University. with the same orientation and the input parameters was taken from the recorded data which already registered of that system. The simulated results were published in a previous paper. [1].

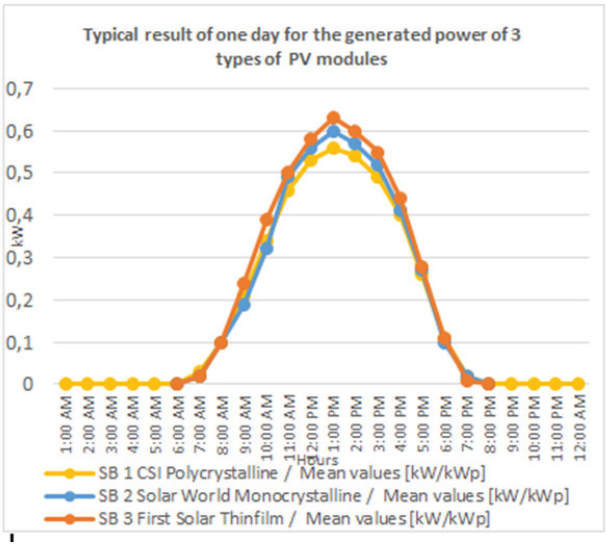

Fig.8 typical result of one day for the generated power (kW) of each of the 3 types of PV modules

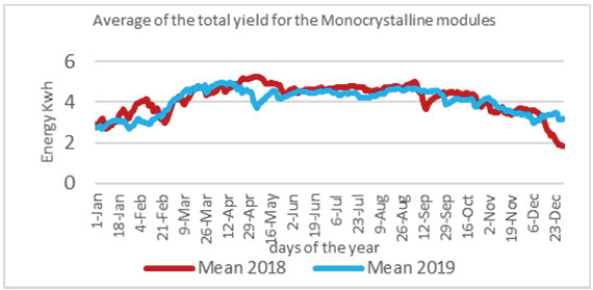

Fig.9 Average of the total yield for the Monocrystalline modules for the years 2018, 2019

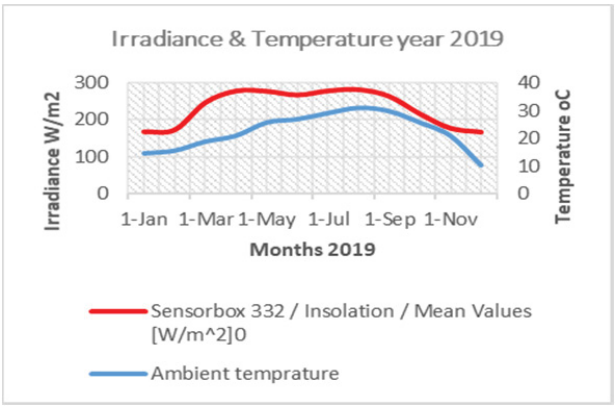

Fig.10 Irradiance & ambient Temperatures results for the year 2019

All input parameters are the real parameters to simulate real conditions applied to the implemented PV system to make the comparison between the simulated output data after applying the reflectors and the real output data before applying the reflectors are closest to the real situation.

A model of a numerical simulation of a stationary solar field augmented by plane reflectors: optimum design parameters to predict the amount of reflected irradiance from the reflector was used based on the dimension of the reflector rational with the dimension of the PV module. Fig. 11. [23]

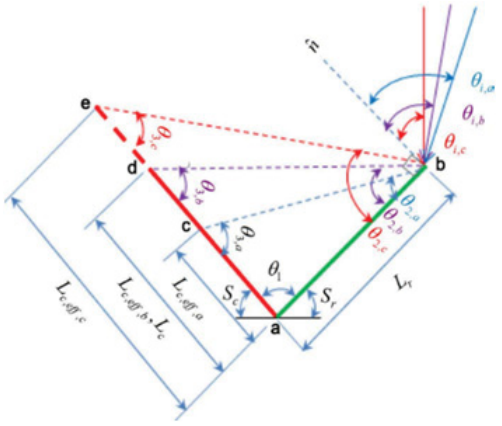

Fig.11 Incidence beam of solar radiation onto the reflector and the PV panel (red arrows), Reflected from the reflector onto the PV panel (blue arrows)

I. Solar Irradiance components calculation

To calculate the diffused irradiance from the reflector:

for total irradiances ($I^t_{c,\ T}$) that strike the PV module's surface, expressed as:

$$I^t_{c.T} = (I^t_b + A^t_i I^t_d)\left[R^t_{b.c} + \frac{L_r}{L_c}\frac{L^t_{c.eff}}{L_c} Q_r R^t_{b.r\to c}\right] + (1 - A^t_i) I^t_d \left[F_{c-sky} + \frac{L_r}{L_c} Q_r F_{r-sky} F_{c-r}\right] \quad (20)$$

where:

$R^t_{b.c}$. $R^t_{b.r\to c}$ are the geometric factors, Q_r is the reflectivity of the reflector,= Reflectivity can be calculated as Q_r = Gr(y)/Gi(y) where Q is the reflectivity= 0.85 for the used reflector., y is the wavelength of the light, G_r is the reflected radiation and G_i is the incident radiation. ≈0.36 percent

$$R^t_{b.c} = \frac{cos\theta^t_{i.c}}{cos\theta^t_z} \ , \ R^t_{b.r\to c} = \frac{cos\theta^t_{i.r\to c}}{cos\theta^t_z} \quad (21)$$

Diffuse reflection is the most common type of reflectivity and occurs when light strikes rough surfaces, such as pavement, foliage, clothing, and vehicles. These surfaces cause the light beams to scatter in all directions. An only a small amount of the light is reflected toward the source. Fig.12.

The values of the reflector height to the PV module height ratio ($\frac{L_r}{L_c}$) and the reflected tilted angle (S_r) are calculating according to the field design parameters: (S_c, $\frac{X}{L_c}$) the collector tilted angle, and the distance separating the rows to the collector height ratio, respectively. the reflector tilt angle is given by:

$$S_r = tan^{-1}\left[\frac{sin\ S_c}{\frac{X}{L} - \cos S_c}\right] \quad (22)$$

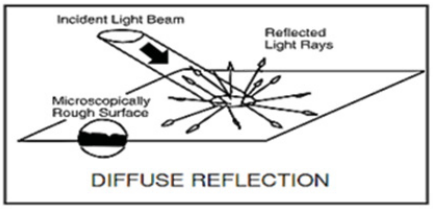

Fig.12. Diffuse Reflection

And the reflector to PV module height ratio is calculated from the following:

$$\frac{L_r}{L_c} = \frac{sin\ S_c}{\sin S_r} \quad (23)$$

The variation of the reflector parameters (S_r, $\frac{L_r}{L_c}$) concerning the solar field parameters (S_c, $\frac{X}{L_c}$) is calculated

F_{c-sky} **:** collector (PV module)-sky view factor:

$$F_{c-sky} = 0 \cdot 5\left[1 + \frac{X}{L_c} - \sqrt{1 + \left(\frac{X}{L_c}\right)^2 - 2\frac{X}{L_c} cosS_s}\right] \quad (24)$$

F_{r-sky} **:** reflector-sky view factor:

$$F_{r-sky} = \frac{\left[\frac{L_r}{L_c} + \frac{X}{L_c} - \sqrt{\left(\frac{L_r}{L_c}\right)^2 + \left(\frac{X}{L_c}\right)^2 - 2\frac{X}{L_c}\frac{L_r}{L_c} cosS_r}\right]}{2\frac{L_r}{L_c}} \quad (25)$$

F_{c-r} **:** collector-reflector view factor **by u**sing the view factor algebra can be presented by:

$$F_{c-r} = 1 - F_{c-sky} \quad (26)$$

By using the above calculations to calculate the new value of the diffused irradiance after using the reflectors, then comparing the result as a diffused extra irradiance as an input with the other recorded environmental data with the implemented PV system after installing the reflectors. Putting under consideration the temperature co-efficient of the PV module which can be assigned as a factor for V_{pv} & I_{PV} for the used panels for each type of the 3 types of the used PV modules. which considered as a very important factor, that, after installing the reflectors to the PV system, an increase in temperature of the module was expected. Then the effect of that expected heat will be calculated and be taken under a consideration.

IV. Rocedures & Practical Results

As a result of the implemented model Fig 13,14,15,16,17

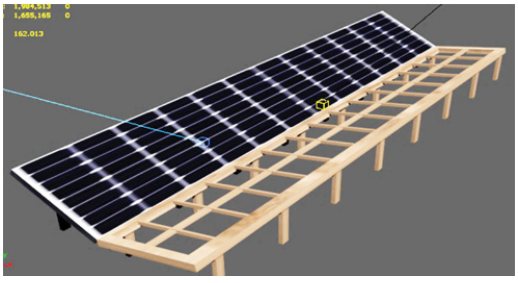

Fig.13 3D design of the reflectors chassis

Fig.14 Building the wooden chassis of the reflectors

Fig.15 Covering the chassis by thin wood layer to attach the reflectors

Fig.16 Fixing of the reflectors

Fig.17 Final stage of the reflectors

The following are just a sample of the whole data which was obtained from the model for one year. The results were the PV panels output power after adding the reflectors to be used in the comparison between the pre-collected data among the previous year before installing the reflector plates.

- A graph of the total PV generated power (P_{pv}) for a normal day in June 2019 before installing the reflectors. Fig.18(a). And the same graph for the same day in June 2020 after installing the reflectors Fig. 18(b). As an input (Irradiance and Ambient temperature) are most close to each other. Also, it can be shown in the graph a detailed reading for each PV type.

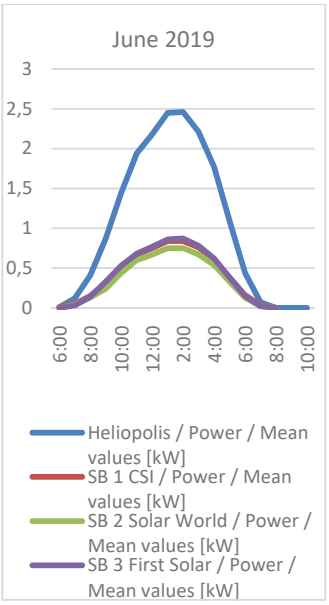

Fig. 18(a)

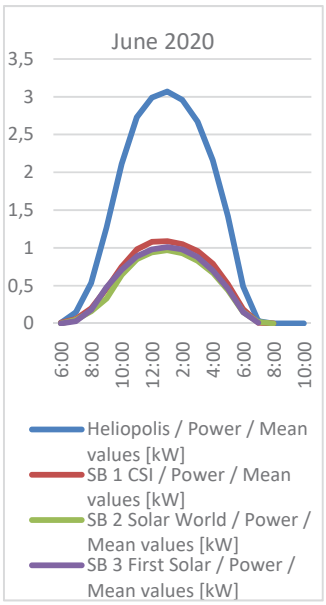

Fig. 18(b)

Fig. 18(a,b) Output before and after installing the reflectors (June). Maximum power ratio= 1.26

- A graph of the total PV generated output power (P_{pv}) for a normal day in October 2019 before installing the reflectors. Fig.19(a). And the same graph for the same day in October 2020 after installing the reflectors Fig.19(b). As an input (Irradiance and Ambient temperature) are most close to each other. Also, a detailed reading for each PV type can be shown in the graph.

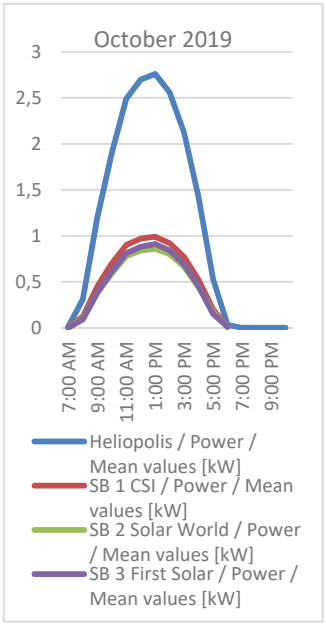

Fig. 19(a)

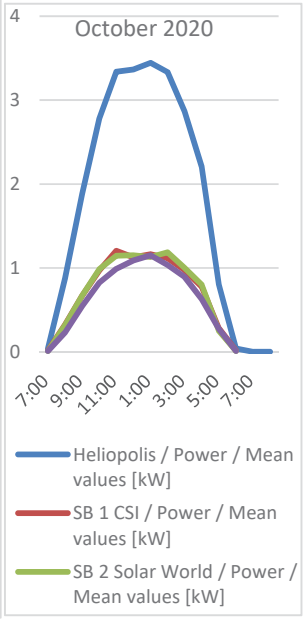

Fig. 19(b)

Fig. 19(a,b) Output before and after installing the reflectors (October). Maximum power ratio= 1.25

- A graph of the total PV generated output power (P_{pv}) for a normal day in Feb. 2020 before installing the reflectors. Fig. 20(a). And the same graph for the same day in Feb. 2021 after installing the reflectors Fig. 20(b). As an input (Irradiance and Ambient temperature) are most close to each other. Also, a detailed reading for each PV type can be shown in the graph.

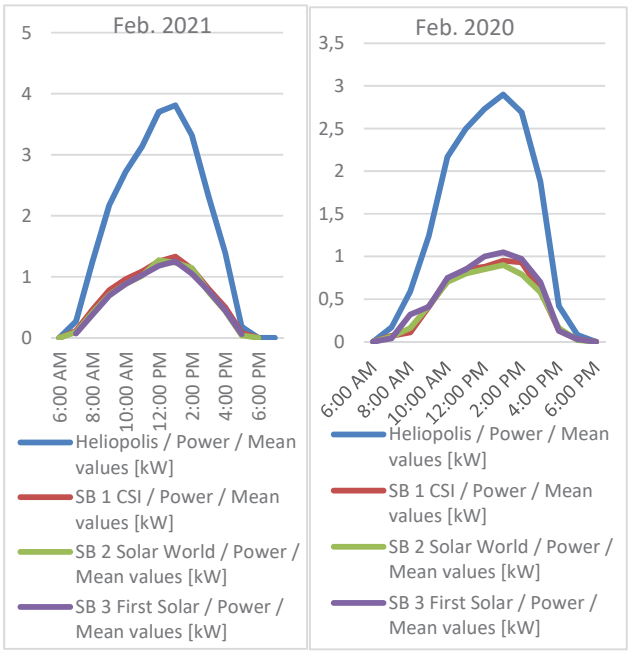

Fig. 20(a) Fig. 20(b)

Fig. 20(a,b) Output before and after installing the reflectors (Feb.). Maximum power ratio= 1.31

- A graph of the total PV generated output power (P_{pv}) for a normal day in May 2020 before installing the reflectors. Fig. 21(a). And the same graph for the same day in May 2021 after installing the reflectors Fig. 21(b). As an input (Irradiance and Ambient temperature) are most close to each other. Also, a detailed reading for each PV type can be shown in the graph.

The data of the output power has been registered for the 3 types of PV panels (Monocrystalline, Polycrystalline, and Thin-film). Samples of the registered data before adding the reflectors are presented as the following. Table II.

TABLE II OUTPUT POWER BEFORE ADDING REFLECTORS FOR THE THREE TYPES OF PV MODULES

Month	Monocrystalline kW	Polycrystalline kW	Thin film kW
January	4.44	5.25	4.34
April	7.71	9.11	7.69
August	6.66	7.89	6.56

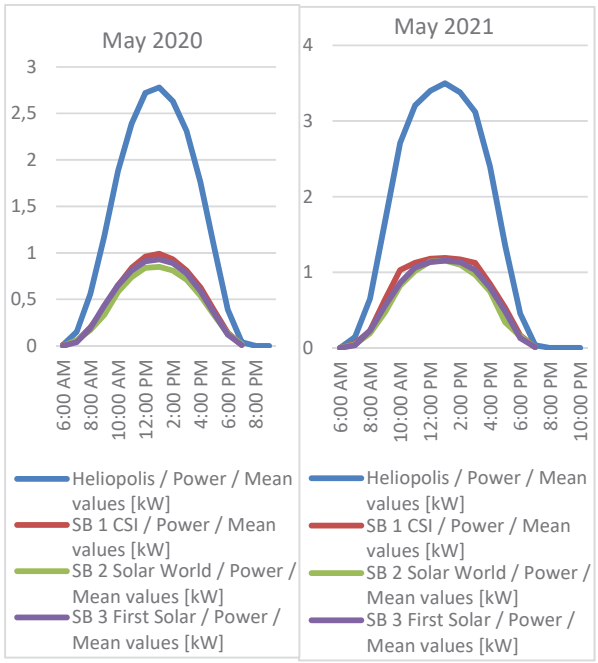

Fig. 21(a) Fig. 21(b)

Fig. 21(a,b) Output before and after installing the reflectors (May). Maximum power ratio= 1.25

Samples of the registered data for the power after adding the reflector was registered for the 3 types of the PV panels are presented as the following. Table III.

TABLE III. OUTPUT POWER AFTER ADDING REFLECTORS FOR THE 3 TYPES OF PV MODULES

Month	Monocrystalline kW	Polycrystalline kW	Thin film kW
January	5.65	6.66	5.41
April	9.57	11.29	9.62
August	8.70	10.26	7.85

A total yield power for one year for all modules before and after adding the reflectors can be presented in the following chart. Fig 22.

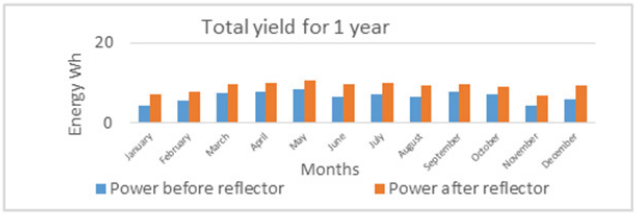

Fig. 22 Total yield for 1 year

Samples of the registered data for the power ratio for the 3 types of PV panels are presented as the following. Table IV.

TABLE IV. POWER RATIO SAMPLES FOR THE 3 TYPES OF PV PANELS

Month	Monocrystalline Power ratio	Polycrystalline Power ratio	Thin film Power ratio
January	1.2709	1.2697	1.2454
April	1.2668	1.2653	1.2755
August	1.3135	1.3076	1.3155

From the above-collected data, a total generated power yield for the 3 types of modules all-over the year before and after applying reflectors are presented in the following Table V.

TABLE V. COLLECTED DATA FOR THE POWER YIELD FOR THE TOTAL OF 3 TYPES OF PV, FOR A TOTAL OF ONE YEAR

	Power before reflectors kW	Power after reflectors kW	Power Ratio
January	4.34	5.63	1.2952
February	5.70	7.15	1.2550
March	7.47	9.21	1.2323
April	7.69	9.82	1.2755
May	8.28	9.49	1.1456
June	6.45	7.99	1.2377
July	6.99	8.72	1.2460
August	6.56	8.60	1.3106
September	7.72	9.72	1.2585
October	7.06	9.02	1.2767
November	4.19	5.49	1.3116
December	5.88	7.42	1.2621

- Monocrystalline and polycrystalline PV modules slightly close in the value of power ratio, monocrystalline PV module is slightly higher in the output power ratio, Fig. 23. but for the whole types, the Thin-film PV module is the most higher in the value of its generated power.

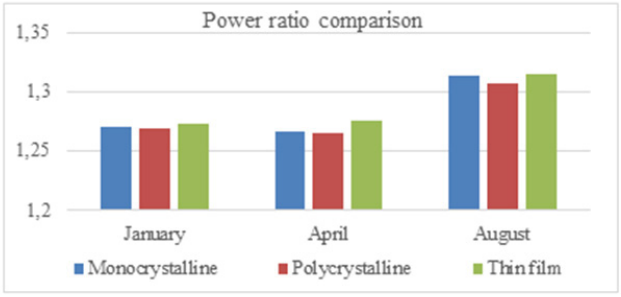

Fig. 23 Samples of the power ratio values for the 3 types of PV panels

IV. CONCLUSION

One of the most effective ways to drive down the cost of PV electricity is to install reflectors attached to the PV panels to harvest more light to it. Which lead to increase practically the output generated power by the range of 21% to 31. This paper approved based on the environmental conditions in Egypt, that both monocrystalline and polycrystalline PV modules slightly close in the value of power ratio, monocrystalline PV module is slightly higher in the output power ratio, but for the whole types, the Thin-film PV module is the most higher in the value of its generated power. The highest average power ratio for the whole 3 types for the Thin-film modules is equal to (1.3158) which means that the output power after installing the reflectors was increased by about 31% from the basic output.

The effect of increasing the temperature could be detected very clearly in the slight decay of the open-circuit voltage value (V_{oc}), which could be neglected if it compared with the increasing of the short circuit current (I_{SC}), the impact of changing temperature dT on maximum power output,P_M= -0.4 % to -0.5% per °C for silicon. That's mean the increasing of the output power is compensating that shortage of the open-circuit voltage as a result of increasing the temperature of the module.

V. FUTURE WORK

- Study the results of using a different material for the reflectors to study the behavior of the generated output power for the 3 types of PV modules. the reflectors could be: 1- White paint high gloss. 2- Tyvek material.

- Separately study the effect of the temperature on each type of the 3 types of PV modules (Monocrystalline, Polycrystalline, and Thin Films) which is a very important parameter for those who are implementing a PV solar system in the hot environmental weather.

- Changing the reflectors angel for a various positions reaching for the optimum angle of the reflectors all over the year.

VI. REFERENCES

[1] Design of an Economic System for Improving the Performance of Three Types of PV Panels Using Solar Reflectors. Ramy Ahmed Faculty of Engineering, Benha University, Benha,, Egypt. Prof. Dr. Ghada Amer Faculty of Engineering, Benha University, Benha, Egypt. Proceeding of The 29TH Conference of FRUCT Association ISSN 2305-7254. 2021.

[2] Performance Comparison of Mirror Reflected Solar Panel with Tracking and Cooling Sheikh Md. Shahin Alam, Dr. A.N.M. Mizanur Rahman Department of Mechanical Engineering Khulna University of Engineering & Technology, 4th International Conference on the Development in the in Renewable Energy Technology (ICDRET) Bangladesh 2016.

[3] Photovoltaic System Performance Enhancement with Non-Tracking Planar Concentrators: Experimental Results and Bi-Directional Reflectance Function (BDRF) Based Modelling Rob W. Andrews, Andrew Pollard, and Joshua M. Pearce IEEE journal of photovoltaics, vol. 5, no. 6, November 2015.

[4] Impact of the solar energy system with and without reflector on home scale batik industry, F Mujaahid, S Febriyanto, R Syahputra, K Purwanto. Department of Electrical Engineering, University of Muhammadiyah Yogyakarta, Indonesia. doi:10.1088/1742-6596/1471/1/012046. 2020

[5] Design and Performance Analysis of Reflectors Attached to Commercial PV Module. N. Palaskar, Deshmukh Department of Mechanical Engineering, Veermata Jijabai Technological Institute Matunga Mumbai, India. S. P. Department of General Engineering, Institute of Chemical Technology Matunga Mumbai, India. International Journal of Renewable Energy Research 4(1):240-245 January 2014

[6] A Study of Optimal Specifications for Light Shelves with Photovoltaic Modules to Improve Indoor Comfort and Save Building Energy. Heangwoo Lee, Xiaolong Zhao, Major in Spatial Design, College of Design, Sangmyung University, Cheonan-si 31066, Chungcheongnam-do, Korea. Janghoo Seo, School of Architecture, Kookmin University, Korea. Int. J. Environ. Res. Public Health 2021, 18, 2574.

[7] Improve the performance of solar modules by reflectors. Naseer K Kasim, Ministry of electricity, Renewable Energy and Environment Center, Iraq. Ahmed F Atwan, and Fadhil Muhmood Eliewi Mustansiriyah University, College of Education, Physics Department, Iraq. IOP Conf. Series: Journal of Physics: Conf. Series **1032** (2018) 012031 doi :10.1088/1742-6596/1032/1/012031. 2018.

[8] Photovoltaic System Performance Enhancement with Non-Tracking Planar Concentrators: Experimental Results and BDRF Based Modelling. Rob W. Andrews ,Andrew Pollard and Joshua M. Pearce Department of Mechanical and Materials Engineering Queen's University, Kingston, Ontario, Canada Department of Materials Science and Engineering and the Department of Electrical and Computer Engineering Michigan Technological University, Houghton, MI, USA 2013.

[9] Solar-concentrating photovoltaic mirror, Arizona state university (USA) PV mirror a solar concentrator mirror incorporating PV cells. Zhengshan Yu. Arizona State University, · Department of lectrical Engineering, USA. 2015.

[10] An experiment of improvement in solar panel efficiency using solar concentration by the number of mirrors. Ranjan Alok et. al; International Journal of Advance Research, Ideas, and Innovations in Technology 2018.

[11] Efficiency Improvement of a Typical Solar Panel with the Use of Reflectors. GDM Pathmika and MV Gamage Department of Mechanical Engineering, Faculty of Engineering, Sri Lanka Institute of Information Technology (SLIIT), 2016.

[12] Enhancement Efficiency of Solar Cell using Simple Mirror Technique. Pooja R. Tandale ,Dr. Sanjay Mohite, P.G. Department of Electronics and Telecommunication, JSPM's JSCOE, Pune, India. 2017.

[13] Increasing the Output Power and Efficiency of Solar Panel by Using Concentrator Photovoltaics (CPV). Muhammad Bilal, Muhammad Naeem Arbab, Muhammad Zain Ul Abideen Afridi, Alishpa Khattak. 2017.

[14] The Solar ATLAS of Egypt. The geo-cradle project received funding from the European union's horizon 2020 research and innovation program under grant agreement no 690133. 2018.

[15] Performance Evaluation of Photovoltaic Solar System with Different Cooling Methods and a Bi-Reflector PV System (BRPVS): An Experimental Study and Comparative Analysis. Muhammad Adil Khan and Hee-Je Kim ,Byeonghun Ko ,Esebi Alois Nyari ,and S. Eugene Park. 2017.

[16] Mirror-Augmented Photovoltaic Designs and Performance. Wei-Chun Lin, Dave Hollingshead, Kara A. Shell, Joseph Karas, Scott A. Brown, Mark Schuetz, Yang Hu, and Roger H. French, Member, IEEE. 2012.

[17] Design and implementation of the solar tracker with reflected mirrors. A.SUNIL & V.PRAVEEN KUMAR Department of Mechanical Engineering, SBIT, Haryana, India. 2016.

[18] Effect of Angle Orientation of Flat Mirror Concentrator on Solar Panel System Output. Assist. Prof Dr. Ali H.AL-Hamadany, Assist. Prof. Dr. Faten Sh. Zain Al-Abideen, Jinnan H. Ali, University of Technology Renewable Energy Research Center, Almustansiriyah University Education College/Physics Department, Baghdad Governorate. 2016.

[19] A Numerical Simulation of a Stationary Solar Field Augmented by Plane Reflector: Optimum Design Parameters. Samer Yassin Alsadi , Yasser Fathi Nassar, Electrical Engineering Department, Faculty of Engineering and Technology, Palestine Technical University-Kadoorie, Tulkarm, Palestine Mechanical Engineering Department, Faculty of Engineering and Technology, Sebha University. July 6, 2017.

[20] A Simple Approach in Estimating the Effectiveness of Adapting Mirror Concentrator and Tracking Mechanism for PV Arrays in the Tropics. M. E. Ya'acob, Myo Than Htay H. Hizam, H. Abdul Rahman, andA.H.M.A.Rahim. Z. Wan Omar.2014

[21] Investigation of soiling effect on different solar mirror materials under Moroccan climate. A.Alami Merrounia , F.Wolfertstetterb , A.Mezrhaba , S.Wilbertb , R.Pitz-Paal. International Conference on Concentrating Solar Power and Chemical Energy Systems. Published by Elsevier Ltd. 2015.

[22] The mathematical model for the power generation from the arbitrarily oriented photovoltaic panel. Qusay Hassan, Marek Jaszczur Estera, Przenzak, Department of Fundamental Research in Energy Engineering, Faculty of Energy and Fuels, AGH University of Science and Technology, Poland. 2017.

[23] Progress in thin film CIGS photovoltaics – Research and development, manufacturing, and applications. Thomas Feurer, Patrick Reinhard, Enrico Avancini, Benjamin Bissig, Johannes Löckinger, Laboratory for Thin Films and Photovoltaics, Empa-Swiss Federal Laboratories for Materials Science and Technology, Ueberlandstrasse 129, 8600 Duebendorf, Switzerland. Published online in Wiley Online Library (wileyonlinelibrary.com). DOI: 10.1002/pip.2811. 3 October 2016

[24] Impact study of operating temperatures and cell layout under different concentration factors in a CPC-PV solar collector in combination with a vertical glass receiver composed by bifacial cells. Chacin, Luís. Loughborough University, UK. Rangel, Simon. FEUP, Porto, (Portugal. Cabral, Diogo, University of Gävle, Faculty of Engineering and Sustainable Development, Department of Building Engineering, Energy Systems and Sustainability Science, Energy Systems and Building Technology. Solar World Congree 2019, 4-7 November, Santiago, Chile. 2020.

[25] Enhancement of some electrical parameters of grid-connected PV solar system using planer concentrators. Naseer K. Kasim, Hazim H. Hussain & Alaa N Abed. Department of Atmospheric Science, Ministry of Electricity/Training and Energy Research Office, Baghdad, Iraq. Energy Sources, Part A: Recovery, Utilization, and Environmental Effects, DOI: 10.1080/15567036.2021.1895374. 2021.

[26] Numerical and Experimental Study of an Asymmetric CPC-PVT Solar Collector. Pouriya Nasseriyan, Department of Mechanical Engineering, Shahid Bahonar University of Kerman, Kerman. Iran. João Gomes, R&D Department, MG Sustainable Engineering AB, Börjegatan 41B, 752 29 Uppsala, Sweden. Energies **2020**, 13, 1669; doi:10.3390/en13071669. 3_ April 2020.